Environmental Science & Technology

Article

pubs.acs.org/est

Fractal Water Quality Fluctuations Spanning the Periodic Table in an Intensively Farmed Watershed

Alice H. Aubert,*[,†,‡,⊗] James W. Kirchner,[§,⊥] Chantal Gascuel-Odoux,[†,‡] Mikael Faucheux,[†,‡] Gérard Gruau,[∥] and Philippe Mérot[†,‡]

[†]Inra, UMR1069, Sol Agro et hydrosystème Spatialisation, FR-35000 Rennes, France

[‡]Agrocampus Ouest, UMR1069, Sol Agro et hydrosystème Spatialisation, FR-35000 Rennes, France

[§]Department of Environmental Systems Science, ETH Zürich, CH-8092 Zürich, Switzerland

[⊥]Swiss Federal Research Institute WSL, CH-8903 Birmensdorf, Switzerland

[∥]Géosciences Rennes, Université de Rennes I, UMR6118, CNRS, FR-35000 Rennes, France

Supporting Information

ABSTRACT: Recently developed measurement technologies can monitor surface water quality almost continuously, creating high-frequency multiparameter time series and raising the question of how best to extract insights from such rich data sets. Here we use spectral analysis to characterize the variability of water quality at the AgrHys observatory (Western France) over time scales ranging from 20 min to 12 years. Three years of daily sampling at the intensively farmed Kervidy-Naizin watershed reveal universal $1/f$ scaling for all 36 solutes, yielding spectral slopes of 1.05 ± 0.11 (mean ± standard deviation). These 36 solute concentrations show varying degrees of annual cycling, suggesting different controls on watershed export processes. Twelve years of daily samples of SO_4, NO_3, and dissolved organic carbon (DOC) show that $1/f$ scaling does not continue at frequencies below 1/year in those constituents, whereas a 12-year daily record of Cl shows a general $1/f$ trend down to the lowest measurable frequencies. Conversely, approximately 12 months of 20 min NO_3 and DOC measurements show that at frequencies higher than 1/day, the spectra of these solutes steepen to slopes of roughly 3, and at time scales shorter than 2−3 h, the spectra flatten to slopes near zero, reflecting analytical noise. These results confirm and extend the recent discovery of universal fractal $1/f$ scaling in water quality at the relatively pristine Plynlimon watershed in Wales, further demonstrating the importance of advective-dispersive transport mixing in catchments. However, the steeper scaling at subdaily time scales suggests additional short-term damping of solute concentrations, potentially due to in-stream or riparian processes.

1. INTRODUCTION

Ever-longer water quality time series have become available in recent decades, both as a result of governmental mandates for environmental monitoring, and from long-term scientific studies. Although environmental managers are mainly interested in determining trends for particular pollutants,[1] researchers use these same data to help in understanding watershed functioning.[2−5] Long-term, high-resolution and multiparameter water quality data are offering new perspectives on watershed processes and their changes over time, including process descriptions at finer time scales.[6,7]

The sampling frequency is a key issue in the design and operation of water quality environmental observatories. The sampling rate creates a temporal filter that highlights some time scales and processes and de-emphasizes others.[7,8] A recent high-frequency sampling campaign at the Plynlimon watershed (Wales) illustrates the impact of sampling rates on hydrological and biogeochemical interpretations of water quality time series. For the past 30 years, the Plynlimon watershed was sampled weekly, but between 2007 and 2009 one of its streams was also sampled every 7 h, revealing a wide range of complex temporal patterns that would not have been expected from the weekly samples.[9−11] Solute concentrations are controlled by different processes operating at different temporal and spatial scales, leading to water quality variations over a range of frequencies. Emerging online measurement technologies can monitor surface water quality almost continuously, with the result that high-frequency water quality time series are becoming available at unprecedented levels of detail.[7]

Those rich data sets enable the use of analyzing tools mining greater information from the data, such as spectral analysis.

Received: August 26, 2013
Revised: December 12, 2013
Accepted: December 13, 2013
Published: December 13, 2013

Spectral analysis has been used in different ways to more precisely characterize hydrological processes: estimating travel time distribution functions,[12−17] identifying periodic signals,[18] and defining the structure of chemical signals to detect underlying properties of the signal.[19,20] Most recently, combined high- and low-frequency sampling at the Plynlimon watershed revealed $1/f$ spectral scaling of streamwater concentrations clear across the periodic table.[19]

The present paper discusses results for spectral analysis of an original data set from the Kervidy-Naizin headwater watershed (France). In contrast to the relatively pristine Plynlimon catchment, Kervidy-Naizin is intensively farmed, with high loadings of nutrients from fertilizers. Here we analyze 3 years of daily concentration data for 36 solutes, 12 years of daily data for nitrate, sulfate, chloride, and dissolved organic carbon (DOC), and about 12 months of 20 min measurements for nitrate and DOC. Our purpose is 2-fold: to determine whether the universal $1/f$ scaling observed at Plynlimon also applies to the intensively farmed Kervidy-Naizin watershed, and to assess the value of quasi-continuous monitoring data for spectral analyses of water quality.

2. STUDY SITE AND METHOD

2.1. Study Site. The Kervidy-Naizin watershed is part of the AgrHys environmental research observatory (references and data are available at http://www7.inra.fr/ore_agrhys_eng/), located in western France (central Brittany; Figure S1, Supporting Information). Water chemistry, hydrology, and meteorology have been intensively monitored since September 1999. In this study, we focus on chemical time series.

The 5 km^2 watershed is drained by a second Strahler order stream, which dries up during some summers. From 2000 to 2012, specific discharge averaged 378 mm/yr and precipitation averaged 815.5 mm/yr, implying mean evapotranspiration (ET) rates of roughly 440 mm/yr or approximately 54% of precipitation; for comparison, annual potential evapotranspiration averaged 705.1 mm/yr. The climate is temperate, with a seasonal pattern such that rainfall is highest in autumn and lowest in late spring.

The watershed's topography is gentle, with maximum slopes of 5% in the Southern part. The watershed is underlain by Brioverian schist, which is considered to be impervious, although it is locally fractured. The schist is capped by up to several meters of unconsolidated weathered material, in which a shallow groundwater table develops, and this weathered material is in turn capped by silty loam soils. The groundwater table varies with position along the hillslope. Wetlands occur near the stream channel, with the water table remaining near the surface most of the year, whereas the water table in the uplands varies seasonally from <1m to ∼3−5m in depth. The groundwater flows from upland to the wetland, contributing to stream discharge[21] and nutrient export.[3,22]

Land use is mostly agricultural, with intensive animal husbandry (in 2010, livestock equivalent units = 13 LSU ha^{-1}). In 2010, the dominant land uses were (in percent of the land surface): 20% cereals, 30% maize, and 20% temporary or permanent pastures. The remaining 30% included minor agricultural crops, wooded plots and hedges, and infrastructure (including roads, pig and hen houses, and other buildings, totaling less than 5% of the land area). The intensive animal husbandry leads to an annual estimated total N surplus of 200 kg N ha^{-1} over the usable agricultural area on average (data from 2010; note that there is great variability among farms).[23] Land use imparts a strong chemical signature in the watershed, with high levels of nitrate (∼74 mg L^{-1}) and chloride (∼34 mg L^{-1}), both in groundwater and streamwater,[24,25] arising mainly from fertilizer applications.

The analysis presented here is based on stream solute concentrations measured at the outlet of the watershed. Anion (NO_3^-, SO_4^{2-}, Cl^-) and dissolved organic carbon (DOC) concentrations have been measured daily since 1999 (12 years), and for 3 years (Sep. 1999−Aug. 2002), alkali metals (Na, K, Rb), alkaline earths (Mg, Ca, Sr, Ba), transition metals (Al, Cr, Mn, Fe, Cu, Zn, Cd, Pb), nonmetals (Si), lanthanides (La, Ce, Pr, Nd, Sm, Eu, Gd, Tb, Dy, Ho, Er, Tm, Yb, Lu), and actinides (Th, U) were also analyzed. Manual grab samples were collected each day at the same hour (5−6 p.m.), filtered (0.2 μm) immediately on site, stored in the dark at 4 °C, and analyzed within 15 days for trace elements by ICP-MS (Agilent series 4500), for anions by ion chromatography (Dionex DX100) and for DOC using a Shimadzu 5050A carbon analyzer. The sampling frequency was reduced to 2−4 times per week during the single hydrologic year of 2002−2003.

To compare these daily measurements with higher frequency monitoring, an in situ UV-spectrometry probe (Spectrolyser, produced by Scan Messtechnik GmbH, Austria) has measured NO_3^- and DOC every 20 min since October 2010. This new device was calibrated in the lab before being installed in stream at the same place where the daily manual samples were collected. The data can thus be continuously cross-checked with the daily manual sampling. This cross-validation led to the culling of 4 months of DOC data, due to biofouling, which caused drift in the UV absorbance.

2.2. Spectral Analysis. Fourier transform power spectra were calculated for each of the time series using the methods of Kirchner and Neal.[19] Any time-domain function $x(t)$ can be converted to an equivalent frequency-domain Fourier transform $X(f)$ (eq 1):

$$X(f) = \int_{-\infty}^{+\infty} x(t)e^{-i2\pi ft}\,dt = \int_{-\infty}^{+\infty} x(t)\cos(2\pi ft)\,dt + \int_{-\infty}^{+\infty} x(t)\sin(2\pi ft)\,dt \quad (1)$$

The complex-valued function $X(f)$ contains both amplitude and phase information. When the phase information can be ignored and only the amplitude information is desired, the Fourier transform is typically multiplied by its complex conjugate, yielding the real-valued spectral power $S_X(f)$ (eq 2).

$$S_X(f) = |X(f)|^2 = \left(\int_{-\infty}^{+\infty} x(t)\cos(2\pi ft)\,dt\right)^2 + \left(\int_{-\infty}^{+\infty} x(t)\sin(2\pi ft)\,dt\right)^2 \quad (2)$$

Spectral power expresses the fluctuation intensity per unit frequency (the power spectral density) and is proportional to the square of the amplitude of the best-fit wave at a given frequency multiplied by record length. Note that many spectral analysis algorithms instead give the square of the amplitude (the so-called periodogram), which is often mistaken for the spectral density but is dimensionally and numerically different. A plot of spectral power against frequency, usually on log−log axes, is termed the power spectrum.

Peaks in the power spectrum indicate periodic cycles, whereas the log−log slope of the power spectrum expresses

the relative strength of short and long wavelengths in the time series, and thus is useful for characterizing the persistence (loosely, the "memory") in the underlying natural processes.[19] Time series with no persistence are characterized by a spectral slope near 0 (termed "white noise", by analogy with the flat spectrum of white light), whereas spectral slopes between 0 and 1 describe weakly persistent (but stationary) time series, and spectral slopes steeper than 1 indicate strongly persistent, nonstationary time series.[19] Therefore, spectral slopes of 1 define the boundary between stationary and nonstationary domains.[19] Time series with spectral slopes of 1 are referred to as $1/f$ noises because their spectral power is inversely proportional to frequency.

All of the time series were visually inspected before analysis, and obvious outliers were removed. Two time series (Al and Pb) were strongly skewed, with a few very high peaks obscuring the rest of the variability (Figure S2, Supporting Information). Those two time series were transformed using the hyperbolic arcsine,[19] which approximates a log transform for high values and a linear transform for smaller values. Special Fourier transform techniques were required for spectral estimation because our time-series were gapped (long summer gaps when the stream dried up and a few intermittent gaps where unreliable measurements were removed) and unevenly spaced (water year 2002−2003 was sampled less intensively). We used an adaptation of Foster's weighted wavelet transform, as described by Kirchner and Neal,[19] to suppress the spectral artifacts associated with the irregular sampling. The highest frequency that can be captured (the Nyquist frequency) for our daily sampling is 0.5/day, and any real-world variability above that frequency will lead to aliasing, and thus to artificial flattening in the measured spectrum. These aliasing artifacts can be severe in $1/f$ noises; to correct for them, we used Kirchner's alias-filtering method,[26] with cutoff and corner frequencies of 2/year and 1460/year, respectively, for the daily data. We did not alias-filter the 20 min data, because the high-frequency tails of those spectra are dominated by measurement noise rather than aliasing.

Kirchner and Neal's [19] spectral methods yield power spectra that are intrinsically averaged over equal intervals of log(frequency), and we estimated the spectral slope by linear regression of these smoothed log−log spectra. The correlations between adjacent estimates of spectral power are accounted for[19] in the standard errors of the spectral slopes (Table 1). Annual cycles were quantified by multiple regression of each time series against $\sin(2\pi\cdot\text{year})$ and $\cos(2\pi\cdot\text{year})$. The R^2 of this multiple regression quantifies the fraction of the total variance that is accounted for by the annual sinusoidal cycle.

3. RESULTS AND DISCUSSION

3.1. Universal Signal Structure vs Diverse Temporal Dynamics. *3.1.1. Diversity vs Similarity of Temporal Dynamics Across the Periodic Table.* From the raw time-series (Figure S2, Supporting Information), several observations can be made. The water year 2000−2001 was extremely wet, whereas the summer/fall of 2001 was characterized by a long dry period. The Lanthanide rare earths (La to Lu) all had similar time-series because the chemical reactivities of these elements are virtually identical (owing to the identical structure of the outer two electron shells), whereas the Actinide rare earths (Th and U) did not show the same concentration peak (particularly the second year). Mn had a temporal pattern somewhat similar to the rare earth elements (REE's) with the same pronounced convex curvature during water year 2000−2001. Na, Mg, Sr, and Ba, along with Si, Cl, and NO_3 (Figure S3 (Supporting Information) and Figure 1), were diluted at high flow, whereas K, Ca, and Rb exhibited peaks associated with both the highest and lowest flows. Most trace metals and the REE's, along with DOC and SO_4 (Figure S3 (Supporting Information) and Figure 1), exhibit positive peaks at high flow.

A further search for signal similarities in the time domain could be the topic of another entire paper and would complement the mechanistic explanations proposed in previous work.[3,24,25,27]

3.1.2. Signal Structure Across the Periodic Table: Universal 1/f Fractal Scaling and Diverse Annual Cycles. The power spectra of the daily sampled solutes are shown in Figure 2. Unsurprisingly, solutes with similar dynamics in the time domain exhibited similar power spectra in the frequency domain. Thus, for example, the spectra of the lanthanide rare earths were visually indistinguishable. All of the power spectra exhibited fractal $1/f$ scaling overall, with spectral slopes averaging 1.05 ± 0.11 (mean ± standard deviation, Table 1). Al and Pb had flatter spectral slopes because the time series were strongly skewed by outliers, but when the time series were hyperbolic arcsine transformed (as shown in Figure 2), their spectral slopes steepened to close to −1. At frequencies below 1/year in the 12-year monitored solutes, the DOC and sulfate spectra flattened, the chloride spectrum continued to exhibit $1/f$ scaling, and the nitrate spectrum reversed slope (indicating markedly lower variability at longer time scales). However, these low-frequency behaviors should be interpreted cautiously, because the uncertainties in this part of the spectrum are relatively large.

The strength of the annual spectral peak varied substantially, reflecting both differences in record length (12 years for SO_4, NO_3, Cl, and DOC vs 3 years for the other analytes) and in the seasonal dynamics of the various solutes. The fraction of the variance explained by an annual sinusoidal cycle varied from 0 to 46% (mean = 20%). Solutes having a less important annual cycle included Pb, Cd, Fe, and Th. The lack of an annual cycle for Pb can be explained by the fact that this element, like Cd, is a constituent of sewage plant sludge and animal manures,[28] both of which are episodically spread onto soils of the study site. Pb, Cd, and Th are also known to be strongly absorbed onto soil particles, leading to possible concentration pulses during intense rainfall events when fine particle transport occurs. This property may contribute to irregular patterns in these elements, because intense rainfall events are rare and episodic. The lack of an annual cycle for Fe can potentially be attributed to the fact that Fe concentrations depend on the redox state of the watershed soils and the redox state varies strongly from year to year, depending on the rainfall distribution and groundwater hydraulic gradient. Conversely, Mn and Si showed the strongest annual cycles. Both elements originate mostly from alteration of bedrock and their export depends strongly on the water table dynamics, which show clear seasonality. Across the periodic table, the strength of the annual cycles is very diverse. No statistically significant cycles were observed other than annual frequencies in the daily Kervidy-Naizin data.

Annual cycles and $1/f$ scaling were also observed in the Plynlimon watershed by Kirchner and Neal (Table 1), although the two watersheds differ markedly, from at least four perspectives. First, although Plynlimon is relatively pristine forest plantation and moorland, Kervidy-Naizin is heavily farmed, with significant impacts on the biogeochemical cycles (particularly of N) via fertilization, plowing, pasture rotation, etc. Second, partly owing to this difference in land use, the two watersheds have

Table 1. Best-Fit Power Law Spectral Slopes (α) and Their Standard Errors (SE) for Kervidy-Naizin Watershed, Compared to Those Reported for the Upper and Lower Hafren at Plynlimon, Wales[a]

	Kervidy-Naizin, daily			Plynlimon, weekly and 7-hourly			
				Upper Hafren		Lower Hafren	
analyte	α	SE (α)	annual cycle (%)	α	SE (α)	α	SE (α)
DOC	1.061	0.035	16	1.177	0.047	1.250	0.073
Cl^-	0.892	0.022	9	1.294	0.054	1.399	0.060
NO_3^-	0.931	0.012	12	1.275	0.074	1.289	0.111
SO_4^{2-}	1.297	0.057	29	1.199	0.035	1.160	0.041
Na	1.082	0.051	16	1.228	0.031	1.347	0.051
K	1.049	0.089	25	1.014	0.032	0.997	0.029
Rb	0.993	0.104	17	0.942	0.021	1.168	0.030
Mg	1.125	0.069	14	1.067	0.060	1.347	0.114
Ca	1.103	0.048	11	0.926	0.063	1.056	0.043
Sr	1.005	0.070	13	0.990	0.064	1.073	0.047
Ba	1.141	0.057	26	0.978	0.034	0.897	0.043
Al	1.108*	0.069*	14*	1.086*	0.042*	0.961*	0.028*
Cr	0.848	0.045	12	1.016	0.030	0.922	0.028
Mn	1.189	0.068	46	1.045	0.027	1.091	0.028
Fe	0.889	0.066	5	1.064	0.044	1.153	0.085
Cu	0.935	0.044	11	1.212	0.060	0.989	0.028
Zn	0.977	0.253	17	0.980	0.025	0.939	0.016
Cd	0.925	0.023	1	0.847	0.034	0.795	0.044
Pb	0.742*	0.046*	0*	0.918	0.015	0.852	0.029
Si	1.140	0.087	40	1.189	0.020	1.288	0.055
La	1.046	0.072	25	1.073	0.037	0.897	0.043
Ce	1.026	0.062	20	1.170	0.049	1.188	0.050
Pr	1.087	0.068	27	1.083	0.055	1.097	0.040
Nd	1.100	0.067	27	NA	NA	NA	NA
Sm	1.097	0.064	27	NA	NA	NA	NA
Eu	1.096	0.071	28	NA	NA	NA	NA
Gd	1.085	0.077	28	NA	NA	NA	NA
Tb	1.087	0.081	27	NA	NA	NA	NA
Dy	1.092	0.073	27	NA	NA	NA	NA
Ho	1.111	0.080	28	NA	NA	NA	NA
Er	1.113	0.077	29	NA	NA	NA	NA
Tm	1.127	0.083	28	NA	NA	NA	NA
Yb	1.131	0.080	31	NA	NA	NA	NA
Lu	1.142	0.074	32	NA	NA	NA	NA
Th	0.994	0.071	5	NA	NA	NA	NA
U	0.944	0.094	11	1.086	0.028	1.133	0.040

[a]Strength of annual cycles for the Kervidy-Naizin time series (% of total variance). Time series that were transformed using the hyperbolic arcsine are denoted by an asterisk.

markedly different baseline chemistry; for example, stream nitrate and chloride concentrations are about 17 and 4 times higher, respectively, at Kervidy-Naizin than at Plynlimon. Third, although the hydrologic cycle at Plynlimon exhibits only weak seasonality (with ET comprising only 20% of the water balance), Kervidy-Naizin has roughly 3-fold less precipitation and a strong seasonal cycle driven by ET (which is roughly 60% of precipitation on an annual basis). Fourth, the topography of Kervidy-Naizin is quite flat, with slopes averaging 5% (compared to 10−20% at Plynlimon) and much more extensive riparian wetlands. Fifth, whereas Kervidy-Naizin is underlain by silty loam soils and relatively impervious metamorphic rocks, Plynlimon is underlain by peats and podzolic soils and deeply fractured metasedimentary rocks with an active fracture flow system. The fractal scaling we have observed at Kervidy-Naizin therefore reinforces the universality of $1/f$ fractal scaling in water quality time series.[13,19] The dominant spectral slopes appear to vary surprisingly little among diverse solutes characterized by different export processes, widely varying chemical reactivity and widely differing natural and anthropogenic sources. Likewise, the spectral slopes appear to be broadly consistent among these two very different watersheds although, of course, they do share some characteristics such as a temperate climate and dominance of subsurface processes in runoff generation.

This occurrence of universal fractal scaling demands a mechanistic explanation. The mechanisms involved must be general across watersheds as diverse as Kervidy-Naizin and Plynlimon, as well as the range of sites analyzed by Godsey et al.[13] It has been previously shown[15,19] that random chemical fluctuations occurring across a landscape can be transformed by downslope advection and dispersion acting across a range of transport length scales to yield $1/f$ time series in streamwater. Downslope advection and dispersion are clearly dominant transport processes in a wide range of watersheds, including Kervidy-Naizin and Plynlimon and also for a wide range of solutes except, perhaps, for those that are very strongly retained

dx.doi.org/10.1021/es403723r | Environ. Sci. Technol. 2014, 48, 930−937

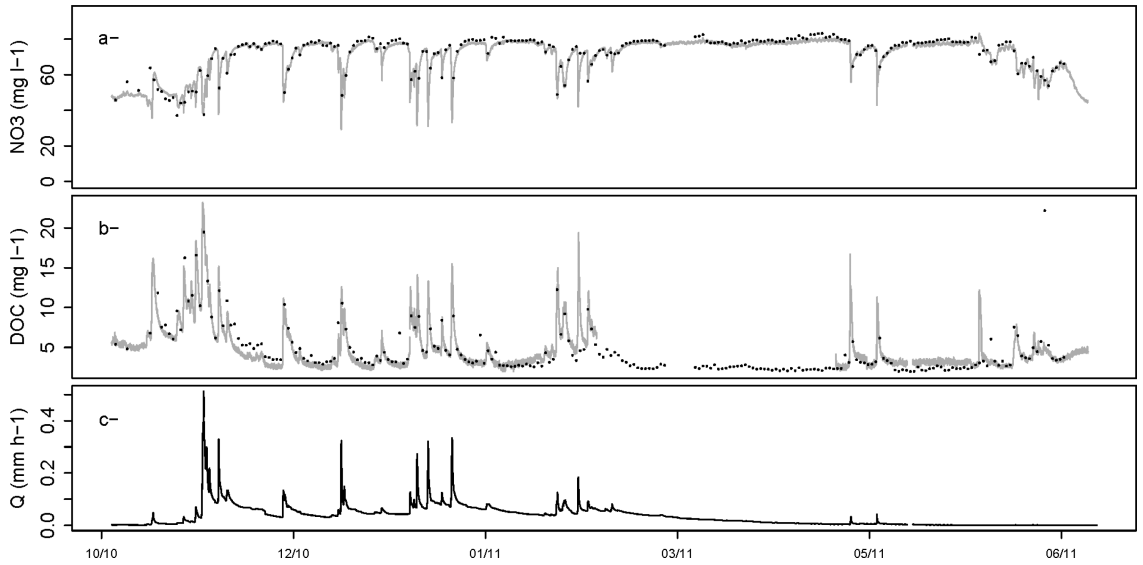

Figure 1. One year (2010–2011) of the 12-year-long daily time series in Kervidy-Naizin for nitrate (a) and dissolved organic carbon (DOC) (b) (instantaneous daily grab samples, black dots) superimposed on 20 min UV-spectrometry measurements (gray lines). In (c), high-frequency discharge measurements are shown for the same period. Hydrologic events shift the relative proportions of shallow and deep groundwater reaching the stream, resulting in enrichment of DOC and dilution of NO_3.

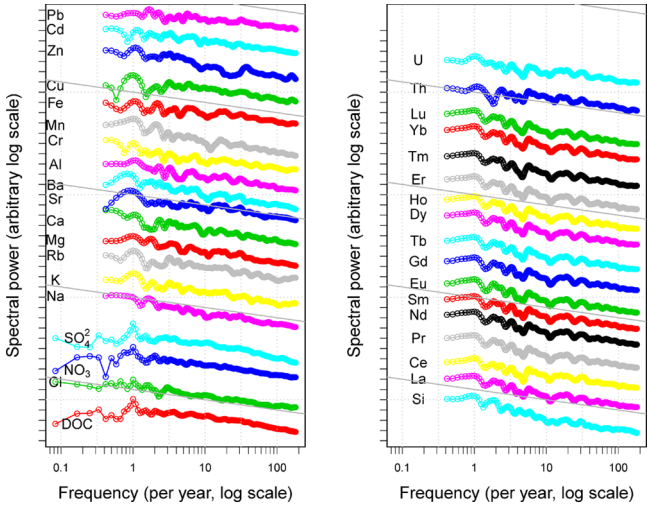

Figure 2. Power for the solutes analyzed in Kervidy-Naizin. Nitrate, chloride, sulfate, and DOC spectra were calculated from 12 years of daily measurements, whereas spectra for all other solutes were calculated from 3 years of daily data. Aluminum and lead time-series were hyperbolic arcsine transformed prior to spectral analysis. The gray lines have a slope of −1 ($1/f$ noise scaling).

by adsorption onto soil particles, or those that are dominantly controlled by in-stream processes. Thus, this mechanism is a plausible candidate for the origin of widespread fractal scaling in stream chemistry time series. As summarized by Kirchner and Neal,[19] other models have also been proposed, which also incorporate various forms of advective-dispersive transport.

Time series that exhibit $1/f$ scaling, like those observed here and at Plynlimon, are "nonself-averaging"; that is, measurements averaged over longer and longer periods of time do not converge to stable averages [ref 19 and references cited therein]. An important implication is that averages and trends in such time series are not nearly as reliable as conventional statistics would suggest.[19,21]

However, it is noteworthy that among the four solutes for which long-term (12-year) time series are available, three (SO_4, NO_3, and DOC) show roughly white-noise scaling at frequencies below about 1/yr, once the obvious annual peaks corresponding to seasonal cycles are factored out (Figures 2 and 3).

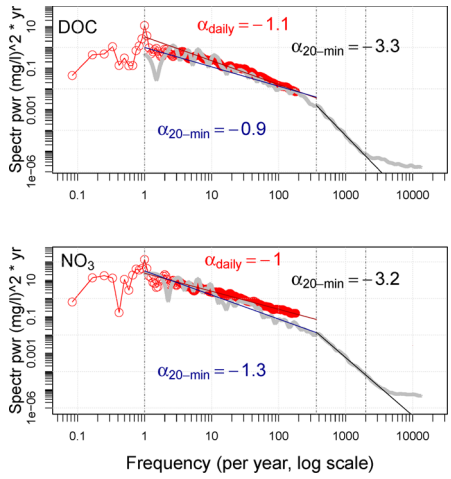

Figure 3. Power spectral density of DOC (upper panel) and nitrate (lower panel) analyzed in Kervidy Naizin on a log–log scale, calculated over a 12-year period from daily time series (red curve) and over one year from 20 min time series (gray curve). The vertical dot-dashed lines mark frequencies of once per year, once per day, and once every 3 h.

This observation suggests that these three solutes should exhibit conventional self-averaging behavior, with more stable means and reliable trends, over time scales much longer than 1 year. For the fourth solute, Cl, $1/f$ scaling extends to the lowest measured frequencies (and thus the longest measured time scales), suggesting that there is no end in sight to its nonself-averaging behavior, even on decadal time scales. The behavior of the other solutes on such long time scales is unknown, because only three years of time series data are available. At Plynlimon,

dx.doi.org/10.1021/es403723r | Environ. Sci. Technol. 2014, 48, 930–937

there is no general trend toward white-noise scaling at the lowest frequencies across 45 elements at two sampling sites [Figure S6 of ref 19], although the authors note that the spectra must become shallower than $1/f$ below some low-frequency limit; otherwise, the variances of the time series would become infinite.

3.2. Insights from the Spectra Obtained from the High Frequency Data. The 20 min time series for NO_3 and DOC showed close agreement with the daily records of the same solutes (Figure 1f–g). The two different sampling frequencies also produce overlapping power spectra, as shown in Figure 3. The fit was remarkably good for DOC, except at frequencies of 1–3/yr where some offset is observed. This can be explained by the fact that (i) a single year was sampled at high frequency (so the power spectrum at frequencies close to 1/yr is highly uncertain) and (ii) the sampled year was characterized by a particularly dry winter. For nitrate, the two spectra exhibit slightly different slopes between frequencies of 10 and 180/yr. This could again reflect the drier-than-normal conditions during the high-frequency sampling, because when rainfall events are scarce, so are the dilution pulses that generate a lot of short-term variation (and hence high-frequency spectral power) in the nitrate time series. Despite these discrepancies, both the daily and 20 min time series show similar $1/f$ scaling in the frequency ranges where they overlap.

However, the 20 min NO_3 and DOC time series show that between time scales of 1 day and 2–3 h, the power spectra steepen from slopes near 1 to slopes near 3. This steepening of the spectrum was anticipated by Kirchner and Neal [19] on theoretical grounds, but was not clearly observable in their spectra, which extended only to time scales of 14 h. This steepening of the spectrum means that at these time scales, the time series is becoming much smoother, with markedly less short-term variability in relation to the longer wavelength fluctuations. Steepening of spectral slopes by 2 (i.e., from 1 to 3) is characteristic of processes that integrate over time. We hypothesize that retention, production, and mixing in the riparian zone or stream could introduce additional fluctuation damping at short time scales (and thus high frequencies), in addition to the $1/f$ damping caused by advection and dispersion during transport to the stream. However, because NO_3 and DOC also respond strongly to stream discharge fluctuations (Figure 1), one must also consider the alternative hypothesis that the shift in spectral slope is driven by steepening of the stream discharge spectrum at similar frequencies. The similarities in the shapes of the NO_3, DOC and discharge spectra lend credibility to this hypothesis (Figure 4).

Both of these hypotheses could be tested using high-frequency sampling of a wider range of solutes. If similar spectral steepening is observed in solutes that respond strongly to stream discharge and those that do not, this would support the first hypothesis over the second. Alternatively, if the spectral steepening is observed only in solutes that are strongly correlated with stream discharge, this would support the second hypothesis over the first. And if spectral steepening occurs in all of the solutes but occurs differently in those that are strongly linked to discharge and those that are not (the steepening occurs in different frequency ranges, for example), this would argue for a combination of both mechanisms.

At time scales shorter than 2–3 h (frequencies of 3000–4000/year), the DOC and NO_3 spectra flatten markedly (Figure 5). This spectral flattening is expected to occur at any frequencies that are high enough that the spectral power of

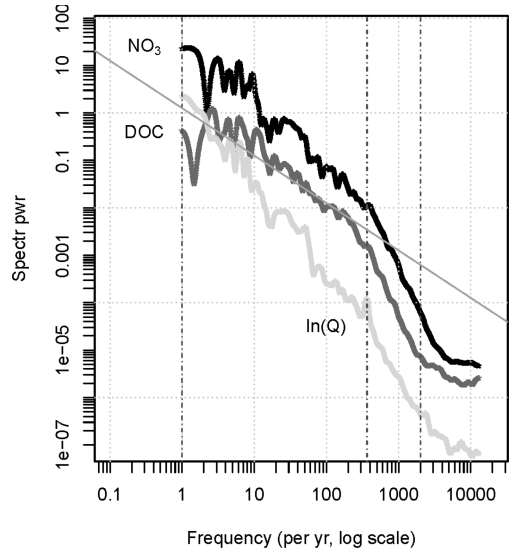

Figure 4. Power spectra of DOC, NO_3 ($(mg/L)^2 \cdot yr$) and ln(Q) ($\log((mm \cdot hr)^2 \cdot yr)$) compared. Vertical dot-dashed lines mark frequencies of once per year, once per day and once every 3 h, to facilitate comparison with Figure 5. Straight gray line indicates slope of −1 ($1/f$ scaling).

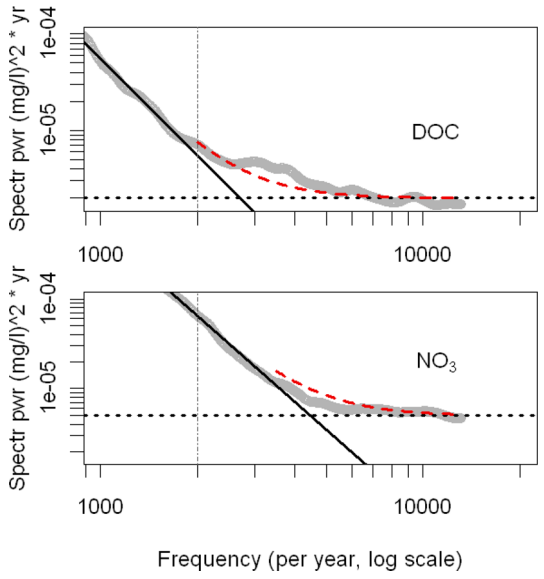

Figure 5. Power spectra of 20 min time series of DOC and nitrate at Kervidy-Naizin, showing only the high-frequency tails. The wide gray line is measured power spectrum. The solid black line is a power-law model fitted to frequencies between 365/year (1 day) and 2000/year (~4 h). The dotted black line is the hypothesized noise floor. The dashed red line is a model for the measured spectrum, obtained by adding the fitted power-law spectrum and the noise floor.

DOC or NO_3 signal becomes small compared to the spectral power of the measurement noise. The slope in the noise tail suggests that the measurement noise may not be spectrally white (i.e., may not have a flat spectrum), but the visible range of frequencies is too small to be sure. The measured spectrum will combine the true real-world signal and the measurement noise, and it will combine them additively if the noise and the real-world signal are uncorrelated with one another.[26] In Figure 5, we model this process by adding a power-law model for the real-world signal (the gray line, fitted to the measured

dx.doi.org/10.1021/es403723r | Environ. Sci. Technol. 2014, 48, 930–937

spectrum between frequencies of 365/year and 2000/year to a white-noise model for the measurement noise (the dotted line). The sum of these two models (the dashed curve) roughly corresponds to the measured spectrum (which, again, will always contain both the signal and noise). The fitted white-noise floors of 5×10^{-6} and 2×10^{-6} ppm^2·yr for nitrate and DOC, respectively, correspond to random measurement errors with standard deviations of ∼0.25 and ∼0.15 ppm, respectively, broadly comparable to the measurement precision specified by the manufacturer (±0.15 and ±1 for NO_3 and DOC, respectively).

Without measuring the noise floor of the sensor system, we cannot definitively exclude the alternative hypothesis that the real-world signal itself exhibits a white-noise tail, although this would be implausible on physical grounds.[19] To our knowledge, the measurement noise power spectra of these sensor systems have not been measured, but we should not necessarily expect them to exhibit white-noise scaling. As long as the real-world signal has a much steeper spectral slope than the instrument noise, there will be a clear separation of scales; in our example, signals at frequencies much higher than 3000−4000/yr (time scales much shorter than 2−3 h) are dominated by noise, whereas at frequencies much lower than this (and therefore time scales much longer than 2−3 h), instrument noise makes a negligible contribution to the measured signal. The separation between these two time scales, however, would be less clear if the real-world signal and the measurement noise exhibited more similar scaling. This points to the importance of knowing the power spectrum of the instrument noise itself, but to our knowledge this is rarely measured (for example, by repeated measurements of blanks and standards).

If measurements at time scales shorter than 2−3 h are dominated by measurement noise, is there any sense in taking measurements at much finer time scales? (Of course the results in any particular case will depend on the frequency at which the signal and noise spectra cross over; we are using 2−3 h just as an example for our data). If the measurement error has a white-noise spectrum, and if higher measurement frequencies do not entail significant additional costs, an optimal strategy would be to measure at the highest possible frequency, and then average these measurements together until the measurement noise (which will tend to average out according to the Central Limit Theorem) has become small compared to the real-world signal. The optimal averaging time scale can be determined from the assumed spectra of the real-world signal and the measurement noise. This approach mimics what already occurs inside many measurement systems, which integrate many noisy instantaneous measurements over a defined time interval when analyzing an individual sample. The benefits of such a strategy, however, will be limited if the measurement noise itself exhibits serial correlation, and thus has a reddened spectrum. This again points to the importance of knowing the spectrum of the measurement noise.

In conclusion, our results demonstrate universal $1/f$ fractal scaling across all the analyzed solutes at Kervidy-Naizin, for frequencies up to 0.5 per day (the Nyquist frequency of our daily sampling). However, the annual cycling differed significantly among the solutes, reflecting differences in their dominant export processes, particularly the strength of their dependence on water table fluctuations or runoff variations. The similarity of the spectral slopes among such diverse solutes (and between catchments as different as Kervidy-Naizin and Plynlimon) emphasizes the need for a general explanation for this phenomenon, such as the advection-dispersion mechanism described by Kirchner et al. [29] and Kirchner and Neal.[19] In-situ UV-spectrometer measurements of DOC and NO_3 at a 20 min frequency gave time series and spectra that were consistent with those from daily sampling but also revealed new information: the spectral slopes steepened markedly between frequencies of once per day and every 3h, and above frequencies of 1/3h, the signal was dominated by measurement noise. A 12-year daily Cl time series showed $1/f$ scaling throughout its entire range, whereas similar long-term records for DOC, NO_3, and SO_4 exhibited white-noise scaling at frequencies below roughly 1/year. Thus, although our results argue for the generality of fractal $1/f$ scaling of stream chemistry at time scales of years to days, they also point to deviations from $1/f$ scaling for some solutes at both long and short wavelengths.

■ ASSOCIATED CONTENT

Supporting Information

A figure of Kervidy-Naizin study site (S1) as well as figures of the raw time series of all 3-year monitored solutes (S2) and all 12-year monitored solutes (S3). The chemistry and discharge data set are also made available. This material is available free of charge via the Internet at http://pubs.acs.org.

■ AUTHOR INFORMATION

Corresponding Author

*A. H. Aubert. E-mail: alice.aubert@rennes.inra.fr.

Present Address

⊗Alice H. Aubert.; INRA-Agrocampus Ouest; UMR SAS 1069; 65, rue de Saint Brieuc CS84215; FR-35042 Rennes Cedex, France

Notes

The authors declare no competing financial interest.

■ ACKNOWLEDGMENTS

We would like to thank all the persons performing the analysis and the field work from both Géosciences (University of Rennes1) and Sol Agro et Hydrosystème Spatialisation (Inra−Agrocampus Ouest): Patricia Madec, Patrice Petitjean, Mikael Faucheux, Yannick Fauvel, Yannick Hamon, and Martine Lecoz-Boutnik, as well as our daily sampler Jean-Paul Guillard. We thank all the Plynlimon team for making their data available, and thank Inra and CNRS for funding the Kervidy-Naizin observatory watershed. We thank the SOERE-RBV network for supporting critical zone research in France.

■ ABBREVIATIONS

DOC	dissolved organic carbon
UV	ultraviolet
REE	rare earth elements
ET	evapotranspiration

■ REFERENCES

(1) Bouraoui, F.; Grizzetti, B. Long term change of nutrient concentrations of rivers discharging in European seas. *Sci. Total Environ.* **2011**, *409* (23), 4899−4916.

(2) Gascuel-Odoux, C.; Aurousseau, P.; Durand, P.; Ruiz, L.; Molenat, J. The role of climate on inter-annual variation in stream nitrate fluxes and concentrations. *Sci. Total Environ.* **2010**, *408* (23), 5657−66.

(3) Molenat, J.; Gascuel-Odoux, C.; Ruiz, L.; Gruau, G. Role of water table dynamics on stream nitrate export and concentration. in agricultural headwater catchment (France). *J. Hydrol.* **2008**, *348* (3−4), 363−378.

(4) Mulholland, P. J.; Hill, W. R. Seasonal patterns in streamwater nutrient and dissolved organic carbon concentrations: Separating catchment flow path and in-stream effects. *Water Resour. Res.* **1997**, *33* (6), 1297−1306.
(5) Zhang, Y. K.; Schilling, K. Temporal variations and scaling of streamflow and baseflow and their nitrate-nitrogen concentrations and loads. *Adv. Water Resour.* **2005**, *28* (7), 701−710.
(6) Schwientek, M.; Osenbruck, K.; Fleischer, M. Investigating hydrological drivers of nitrate export dynamics in two agricultural catchments in Germany using high-frequency data series. *Environ. Earth Sci.* **2013**, *69* (2), 381−393.
(7) Gunnerson, C. G. Optimizing sampling intervals in tidal estuaries. *J. Sanit. Eng. Div., Am. Soc. Civ. Eng.* **1966**, *92* (SA2), 103−125.
(8) Kirchner, J. W.; Feng, X.; Neal, C.; Robson, A. J. The fine structure of water-quality dynamics: the (high-frequency) wave of the future. *Hydrol. Processes* **2004**, *18* (7), 1353−1359.
(9) Neal, C.; Reynolds, B.; Norris, D.; Kirchner, J. W.; Neal, M.; Rowland, P.; Wickham, H.; Harman, S.; Armstrong, L.; Sleep, D.; Lawlor, A.; Woods, C.; Williams, B.; Fry, M.; Newton, G.; Wright, D. Three decades of water quality measurements from the Upper Severn experimental catchments at Plynlimon, Wales: an openly accessible data resource for research, modelling, environmental management and education. *Hydrol. Processes* **2011**, *25* (24), 3818−3830.
(10) Halliday, S. J.; Wade, A. J.; Skeffington, R. A.; Neal, C.; Reynolds, B.; Rowland, P.; Neal, M.; Norris, D. An analysis of long-term trends, seasonality and short-term dynamics in water quality data from Plynlimon, Wales. *Sci. Total Environ.* **2012**, *434* (0), 186−200.
(11) Neal, C.; Reynolds, B.; Rowland, P.; Norris, D.; Kirchner, J. W.; Neal, M.; Sleep, D.; Lawlor, A.; Woods, C.; Thacker, S.; Guyatt, H.; Vincent, C.; Hockenhull, K.; Wickham, H.; Harman, S.; Armstrong, L. High-frequency water quality time series in precipitation and streamflow: From fragmentary signals to scientific challenge. *Sci. Total Environ.* **2012**, *434*, 3−12.
(12) Feng, X.; Kirchner, J. W.; Neal, C. Spectral Analysis of Chemical Time Series from Long-Term Catchment Monitoring Studies: Hydrochemical Insights and Data Requirements. *Water, Air, Soil Pollut.: Focus* **2004**, *4* (2), 221−235.
(13) Godsey, S. E.; Aas, W.; Clair, T. A.; de Wit, H. A.; Fernandez, I. J.; Kahl, J. S.; Malcolm, I. A.; Neal, C.; Neal, M.; Nelson, S. J.; Norton, S. A.; Palucis, M. C.; Skjelkvale, B. L.; Soulsby, C.; Tetzlaff, D.; Kirchner, J. W. Generality of fractal 1/f scaling in catchment tracer time series, and its implications for catchment travel time distributions. *Hydrol. Processes* **2010**, *24* (12), 1660−1671.
(14) Hrachowitz, M.; Soulsby, C.; Tetzlaff, D.; Dawson, J. J. C.; Dunn, S. M.; Malcolm, I. A. Using long-term data sets to understand transit times in contrasting headwater catchments. *J. Hydrol.* **2009**, *367* (3−4), 237−248.
(15) Kirchner, J. W.; Feng, X. H.; Neal, C. Fractal stream chemistry and its implications for contaminant transport in catchments. *Nature* **2000**, *403*, 524−527.
(16) Molenat, J.; Davy, P.; Gascuel-Odoux, C.; Durand, P. Spectral and cross-spectral analysis of three hydrological systems. *Physics and Chemistry of the Earth, Part B: Hydrology, Oceans and Atmosphere* **2000**, *25* (4), 391−397.
(17) Molenat, J.; Gascuel-Odoux, C.; Aquilina, L.; Ruiz, L. Use of gaseous tracers (CFCs and SF6) and transit-time distribution spectrum to validate a shallow groundwater transport model. *J. Hydrol.* **2013**, *480*, 1−9.
(18) Luque-Espinar, J. A.; Chica-Olmo, M.; Pardo-Igúzquiza, E.; García-Soldado, M. J. Influence of climatological cycles on hydraulic heads across a Spanish aquifer. *J. Hydrol.* **2008**, *354* (1−4), 33−52.
(19) Kirchner, J. W.; Neal, C. Universal fractal scaling in stream chemistry and its implications for water quality trend detection. *Proc. Natl. Acad. Sci. U. S. A.* **2013**, *110* (30), 12213−12218.
(20) Shaw, S. B.; Harpold, A. A.; Taylor, J. C.; Walter, M. T. Investigating a high resolution, stream chloride time series from the Biscuit Brook catchment, Catskills, NY. *J. Hydrol.* **2008**, *348* (3−4), 245−256.
(21) Molénat, J.; Gascuel-Odoux, C.; Davy, P.; Durand, P. How to model shallow water-table depth variations: the case of the Kervidy-Naizin catchment, France. *Hydrol. Processes* **2005**, *19* (4), 901−920.
(22) Molenat, J.; Gascuel-Odoux, C. Modelling flow and nitrate transport in groundwater for the prediction of water travel times and of consequences of land use evolution on water quality. *Hydrol. Processes* **2002**, *16* (2), 479−492.
(23) Akkal, N., Description des systèmes d'exploitation du bassin versant de Kervidy-Naizin. *NitroEurope IP* internal report, 2010; p 71.
(24) Aubert, A. H.; Gascuel-Odoux, C.; Gruau, G.; Akkal, N.; Faucheux, M.; Fauvel, Y.; Grimaldi, C.; Hamon, Y.; Jaffrezic, A.; Lecoz Boutnik, M.; Molenat, J.; Petitjean, P.; Ruiz, L.; Merot, P. Solute transport dynamics in small, shallow groundwater-dominated agricultural catchments: insights from a high-frequency, multisolute 10 yr-long monitoring study. *Hydrol. Earth Syst. Sci.* **2013**, *17* (4), 1379−1391.
(25) Dia, A.; Gruau, G.; Olivie-Lauquet, G.; Riou, C.; Molenat, J.; Curmi, P. The distribution of rare earth elements in groundwaters: Assessing the role of source-rock composition, redox changes and colloidal particles. *Geochim. Cosmochim. Acta* **2000**, *64* (24), 4131−4151.
(26) Kirchner, J. W. Aliasing in 1/f(alpha) noise spectra: origins, consequences, and remedies. *Phys. Rev. E* **2005**, *71* (066110), 1−16.
(27) Lambert, T.; Pierson-Wickmann, A.-C.; Gruau, G.; Thibault, J.-N.; Jaffrezic, A. Carbon isotopes as tracers of dissolved organic carbon sources and water pathways in headwater catchments. *J. Hydrol.* **2011**, *402* (3−4), 228−238.
(28) Nicholson, F. A.; Chambers, B. J.; Williams, J. R.; Unwin, R. J. Heavy metal contents of livestock feeds and animal manures in England and Wales. *Bioresour. Technol.* **1999**, *70* (1), 23−31.
(29) Kirchner, J. W.; Feng, X.; Neal, C. Catchment-scale advection and dispersion as a mechanism for fractal scaling in stream tracer concentrations. *J. Hydrol.* **2001**, *254*, 82−101.